Supplementary materials for New Journal of Chemistry

Two energetic complexes incorporating 3,5-dinitrobenzoic acid and azole ligands: Microwave-assisted syntheses, favorable detonation properties, insensitivity and effects on the thermal decomposition of RDX

Qi Yang*, Jing Ge, Qibing Gong, Xiaxia Song, Jinwen Zhao, Qing Wei, Gang Xie, Sanping Chen* , Shengli Gao

Key Laboratory of Synthetic and Natural Functional Molecule Chemistry of Ministry of Education, College of Chemistry and Materials Science, Northwest University, Xi'an, Shaanxi 710127, China

Table of contents

Table S1 Selected bond distances (Å) and angles (°) for **1** and **2**
Table S2 Hydrogen bonding interactions in **1**
Fig. S1 XRPD curves for complex **1**
Fig. S2 XRPD curves for complex **2**
Fig. S3 TG curve of complex **1**
Fig. S4 TG curve of complex **2**
Fig. S5 DSC curve of complex **1** under the linear heating rate of 5 °C/min
Fig. S6 DSC curve of complex **1** under the linear heating rate of 10 °C/min
Fig. S7 DSC curve of complex **1** under the linear heating rate of 15 °C/min
Fig. S8 DSC curve of complex **1** under the linear heating rate of 20 °C/min
Fig. S9 DSC curve of complex **2** under the linear heating rate of 5 °C/min
Fig. S10 DSC curve of complex **2** under the linear heating rate of 10 °C/min
Fig. S11 DSC curve of complex **2** under the linear heating rate of 15 °C/min
Fig. S12 DSC curve of complex **2** under the linear heating rate of 20 °C/min
Fig. S13 DSC curve of complex **1** + RDX under the linear heating rate of 5 °C/min
Fig. S14 DSC curve of complex **1** + RDX under the linear heating rate of 10 °C/min
Fig. S15 DSC curve of complex **1** + RDX under the linear heating rate of 15 °C/min
Fig. S16 DSC curve of complex **1** + RDX under the linear heating rate of 20 °C/min
Fig. S17 DSC curve of complex **2** + RDX under the linear heating rate of 5 °C/min
Fig. S18 DSC curve of complex **2** + RDX under the linear heating rate of 10 °C/min
Fig. S19 DSC curve of complex **2** + RDX under the linear heating rate of 15 °C/min
Fig. S20 DSC curve of complex **2** + RDX under the linear heating rate of 20 °C/min

*Corresponding author: Prof. Qi Yang
E-mail:yangqi@nwu.edu.cn

Table S1 Selected bond distances (Å) and angles (°) for **1** and **2**

$Co(TO)_2(DNBA)_2(H_2O)_2$ (**1**)			
Co(1)-N(1)	2.095(3)	Co(1)-O(7)	2.116(2)
Co(1)-O(8)	2.115(2)		
N(1)-Co(1)-N(1)	180.0(2)	N(1)#1-Co(1)-O(8)	92.32(9)
O(8)-Co(1)-O(8)	180.0(2)	N(1)-Co(1)-O(7)#1	91.02(7)
N(1)#1-Co(1)-O(7)	88.98(7)	O(8)-Co(1)-O(7)#1	87.57(8)
O(8)#1-Co(1)-O(7)	92.43(8)	N(1)-Co(1)-O(7)	88.98(7)
N(1)#1-Co(1)-O(7)	91.02(7)	O(8)-Co(1)-O(7)	92.43(8)
O(8)#1-Co(1)-O(7)	87.57(8)	Co(1)-O(8)-H(8W)	100(3)
Cu(HTZA)(DNBA) (**2**)			
Cu(1)-O(7)#1	1.959(4)	O(1)-Cu(1)-O(6)	88.3(2)
Cu(1)-O(8)#1	1.960(5)	O(7)#1-Cu(1)-N(4)#2	100.56(19)
Cu(1)-O(1)	1.969(5)	O(8)#1-Cu(1)-N(4)#2	95.3(2)
Cu(1)-O(6)	1.985(4)	O(1)-Cu(1)-N(4)#2	97.5(2)
Cu(1)-N(4)#2	2.159(5)	O(7)#1-Cu(1)-Cu(1)#1	80.55(13)
O(7)#1-Cu(1)-O(8)#1	89.4(2)	O(8)#1-Cu(1)-Cu(1)#1	81.07(15)
O(7)#1-Cu(1)-O(1)	89.5(2)	O(1)-Cu(1)-Cu(1)#1	86.12(14)
O(8)#1-Cu(1)-O(1)	167.15(19)	O(6)-Cu(1)-Cu(1)#1	86.70(13)
O(7)#1-Cu(1)-O(6)	167.18(18)	N(4)#2-Cu(1)-Cu(1)#1	176.18(15)
O(8)#1-Cu(1)-O(6)	90.0(2)		

Symmetry transformations used to generate equivalent atoms: #1=-x+1,-y,-z; #2=-x+1,-y+1,-z

Table S2 Hydrogen bonding interactions in **1**

D—H···A	H···A (Å)	D···A (Å)	D—H···A (Å)	D—H···A (°)
N(2)-H(2)...O(8)#2	0.86	2.21	2.844(3)	130.6
N(2)-H(2)...O(7)	0.86	2.55	2.980(3)	112.1
O(8)-H(8WB)...O(1)#3	0.83(4)	1.99(4)	2.759(3)	155(4)
O(8)-H(8WA)...O(6)	0.82(4)	1.77(4)	2.568(3)	164(4)

Symmetry transformations used to generate equivalent atoms:

#1 -x+1,-y+1,-z #2 x+1,y,z #3 x-1,y,z

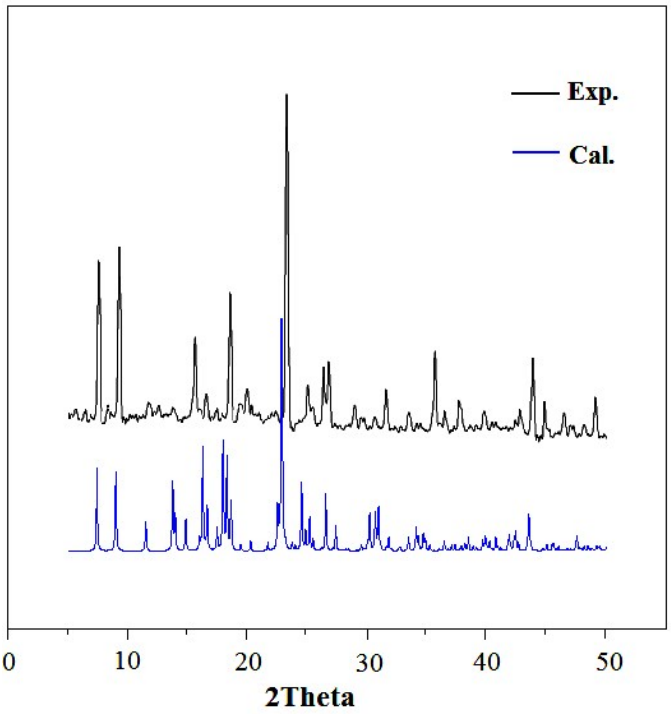

Fig. S1 XRPD curves for complex **1**.

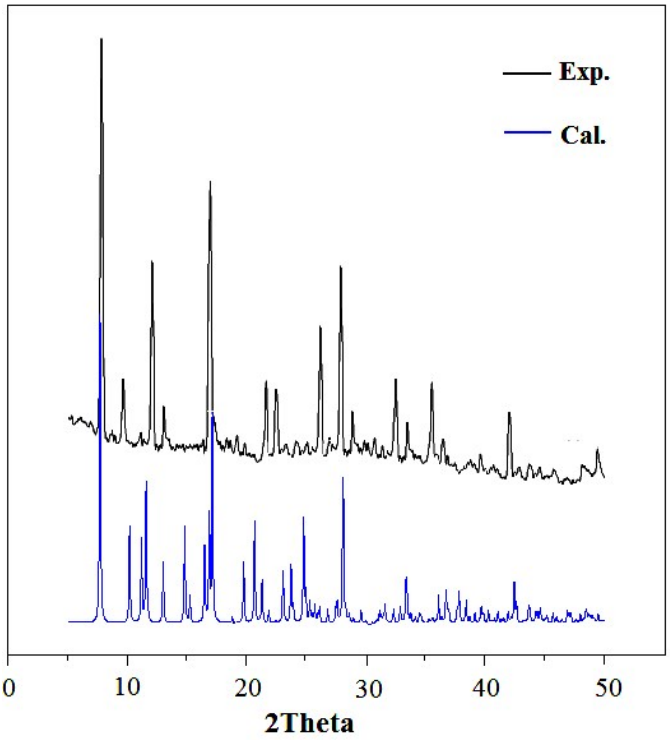

Fig. S2 XRPD curves for complex **2**.

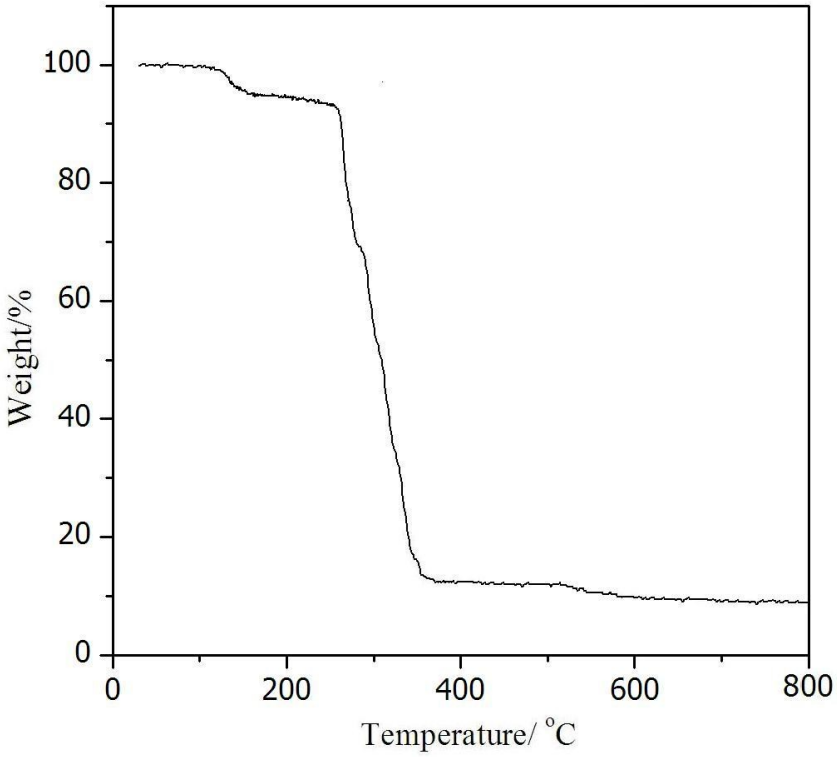

Fig. S3 TG curve of complex **1**

Fig. S4 TG curve of complex **2**

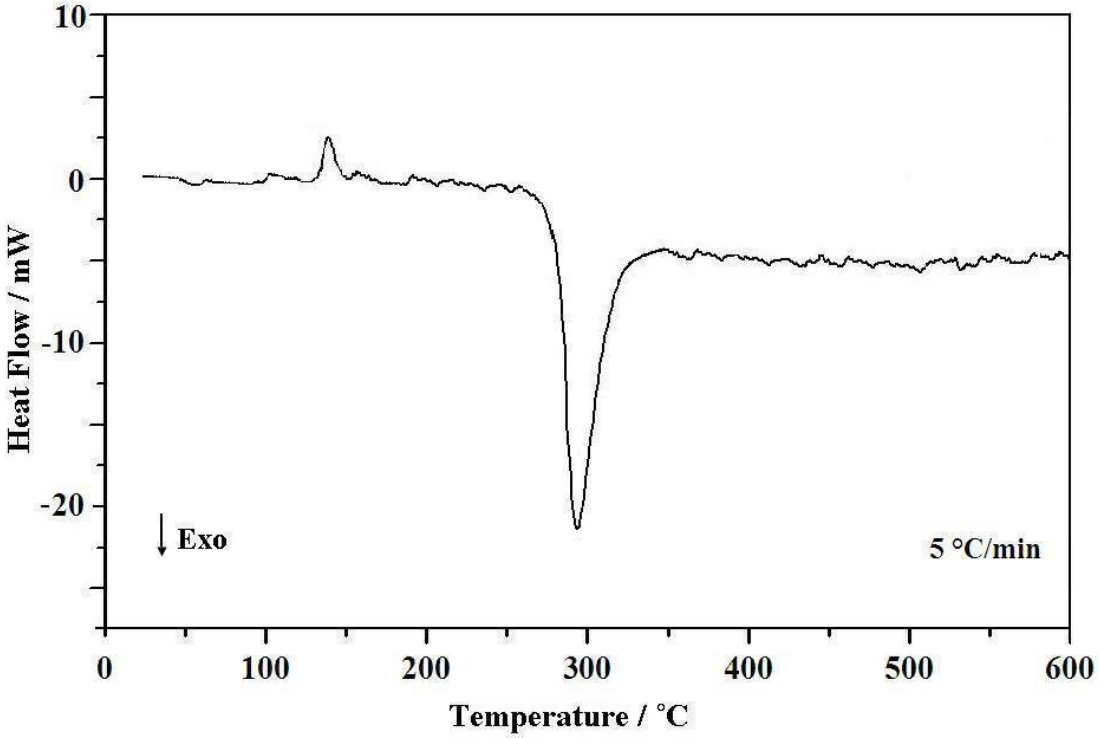

Fig. S5 DSC curve of complex **1** under the linear heating rate of 5 °C/min

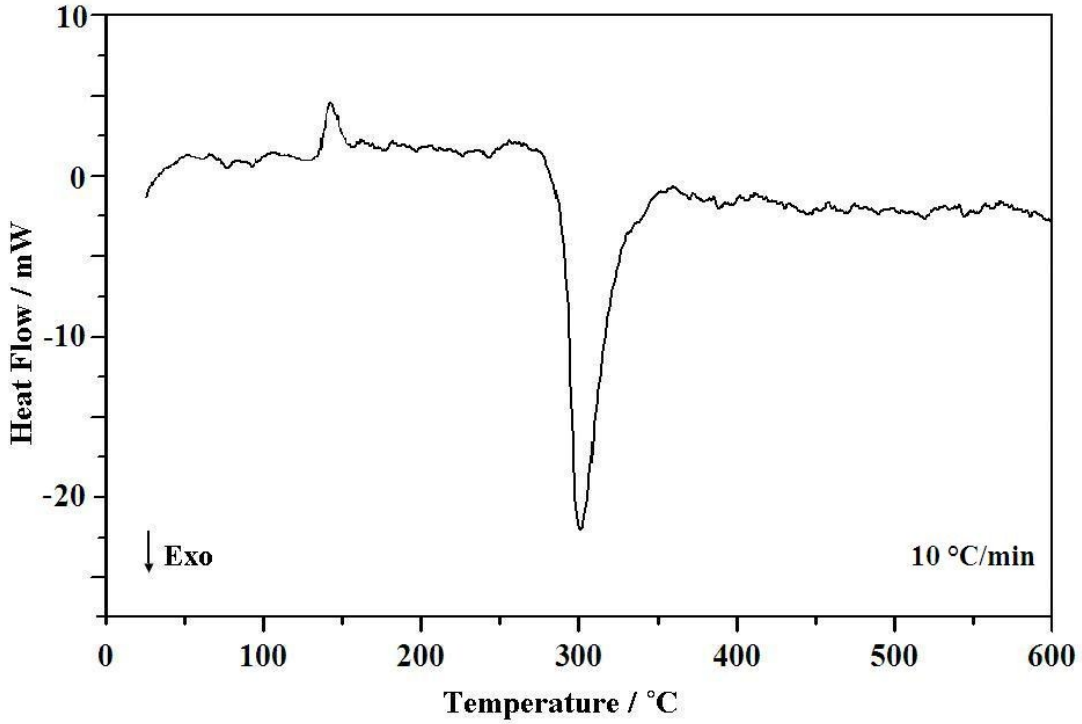

Fig. S6 DSC curve of complex **1** under the linear heating rate of 10 °C/min

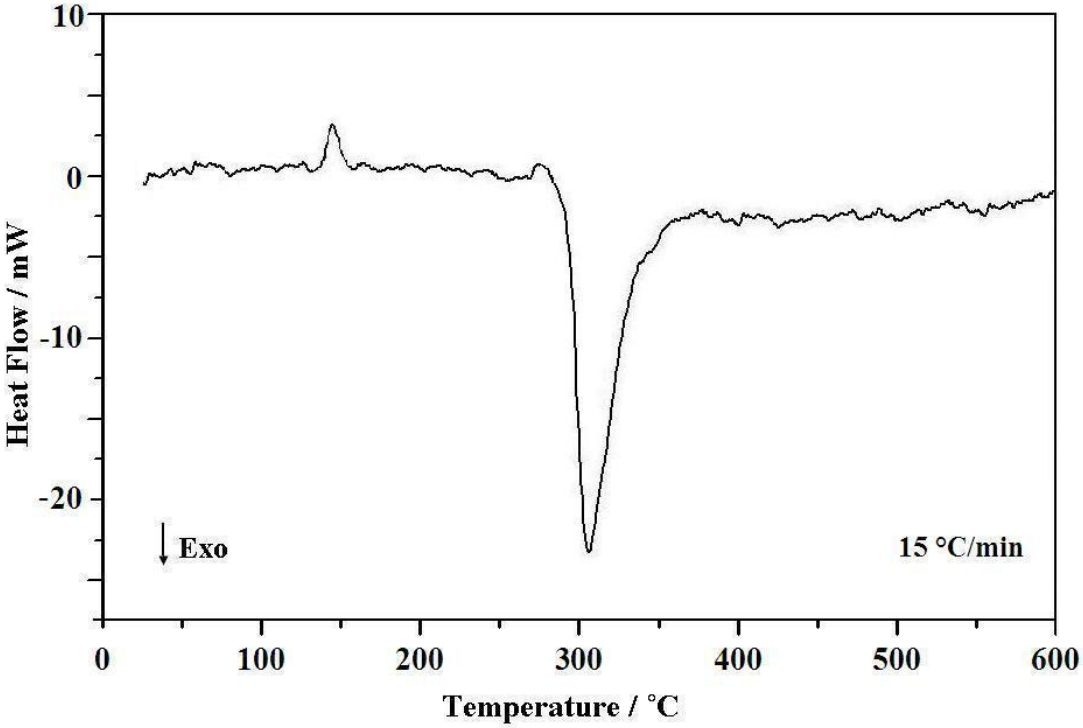

Fig. S7 DSC curve of complex **1** under the linear heating rate of 15 °C/min

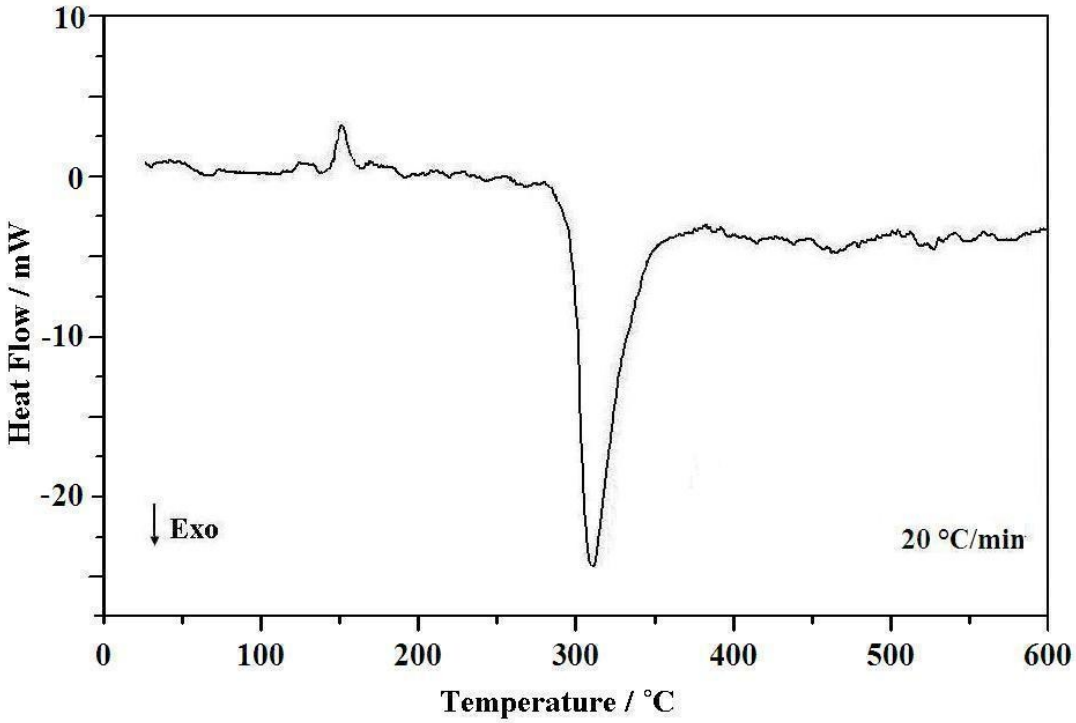

Fig. S8 DSC curve of complex **1** under the linear heating rate of 20 °C/min

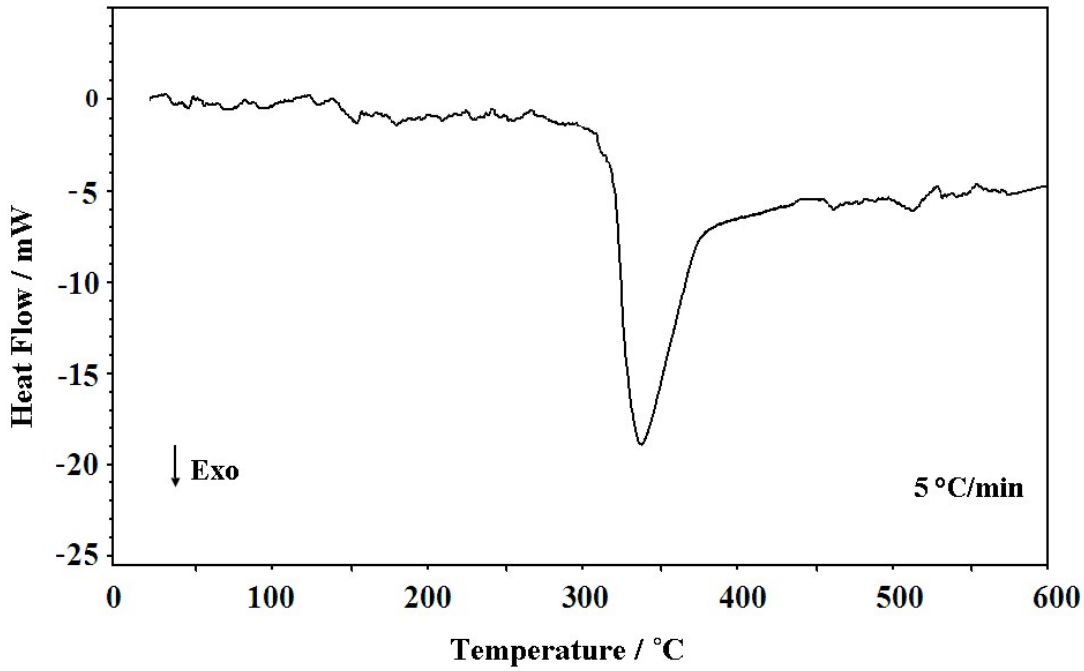

Fig. S9 DSC curve of complex **2** under the linear heating rate of 5 °C/min

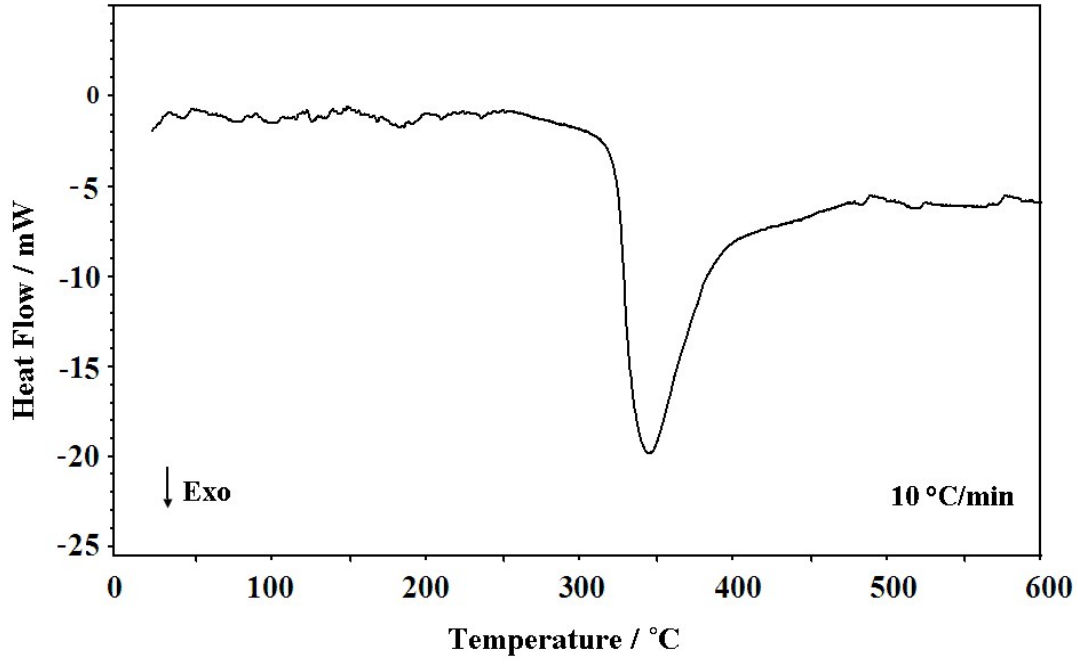

Fig. S10 DSC curve of complex **2** under the linear heating rate of 10 °C/min

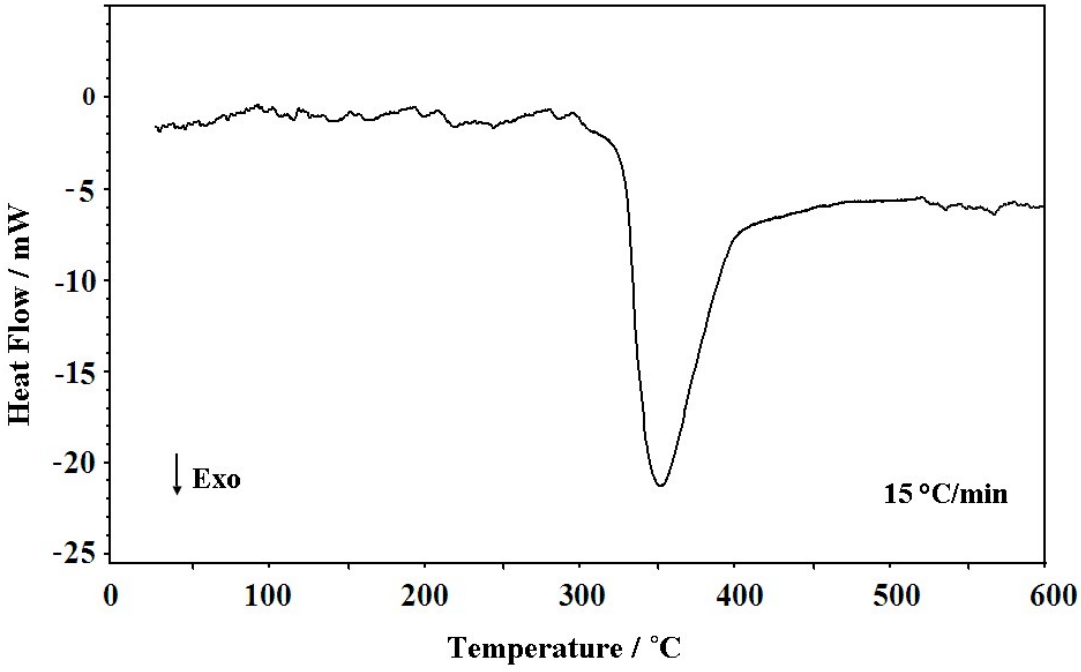

Fig. S11 DSC curve of complex **2** under the linear heating rate of 15 °C/min

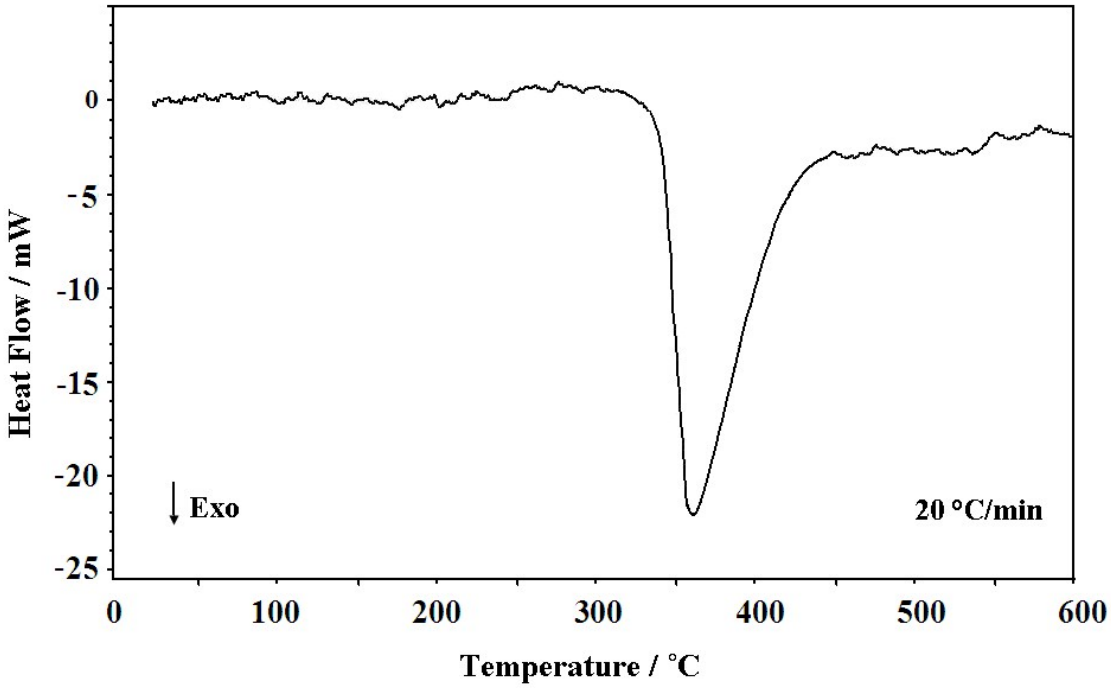

Fig. S12 DSC curve of complex **2** under the linear heating rate of 20 °C/min

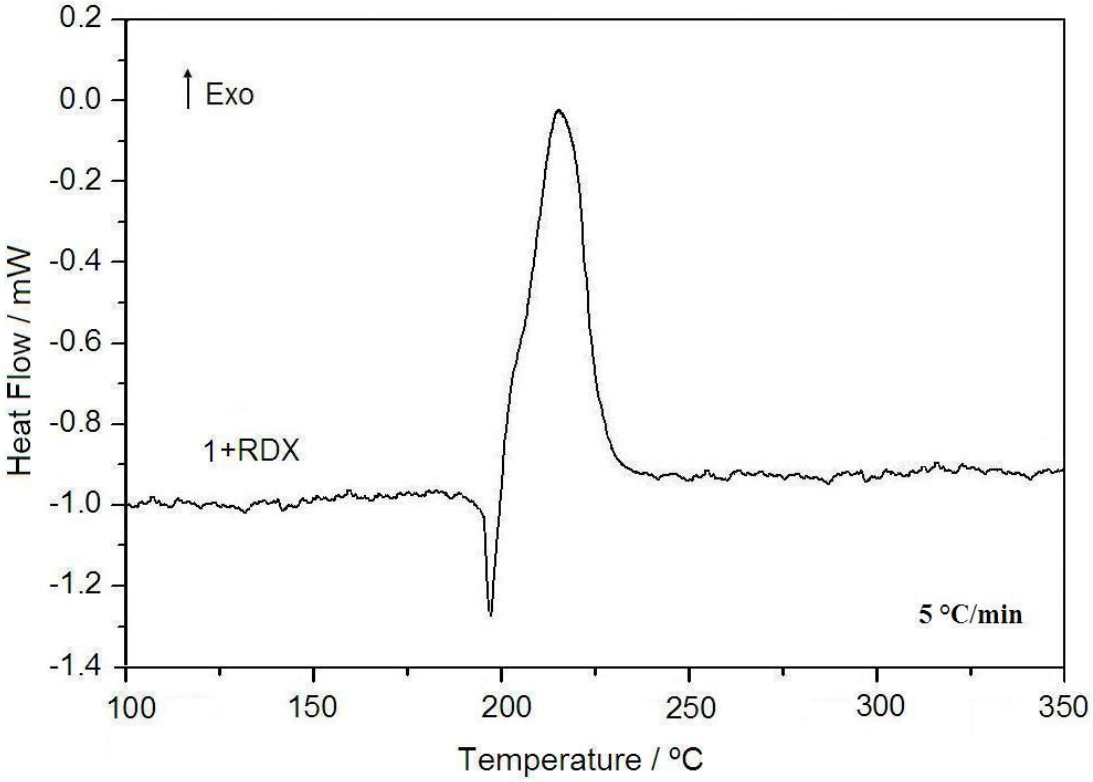

Fig. S13 DSC curve of complex **1** + RDX under the linear heating rate of 5 °C/min

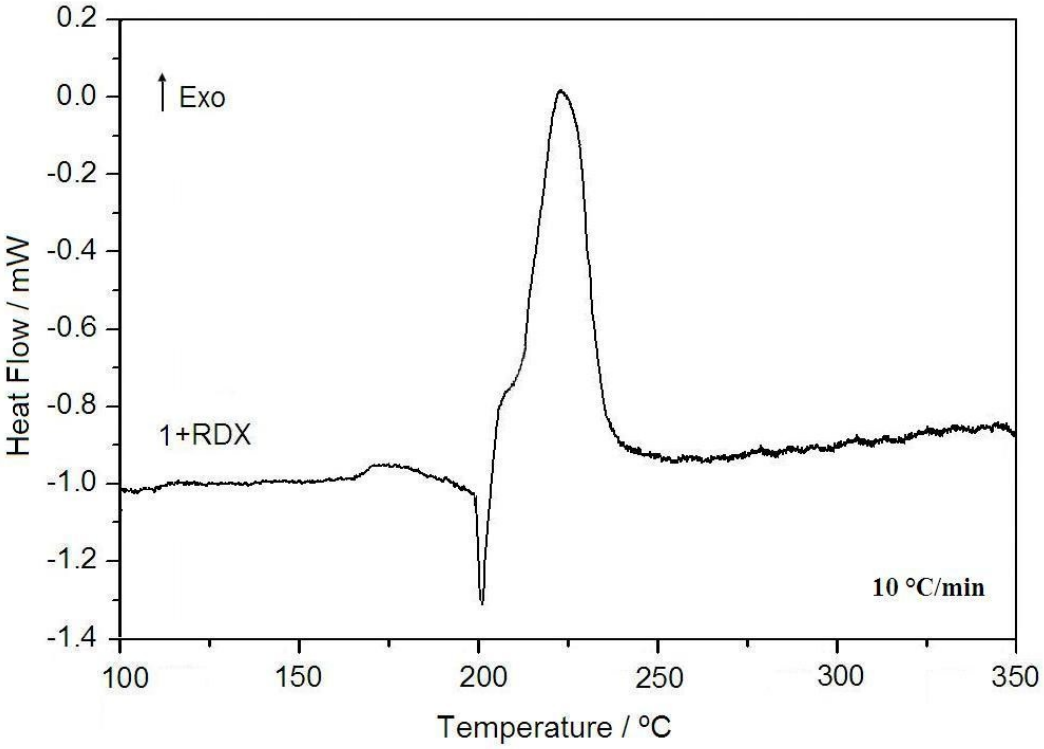

Fig. S14 DSC curve of complex **1** + RDX under the linear heating rate of 10 °C/min

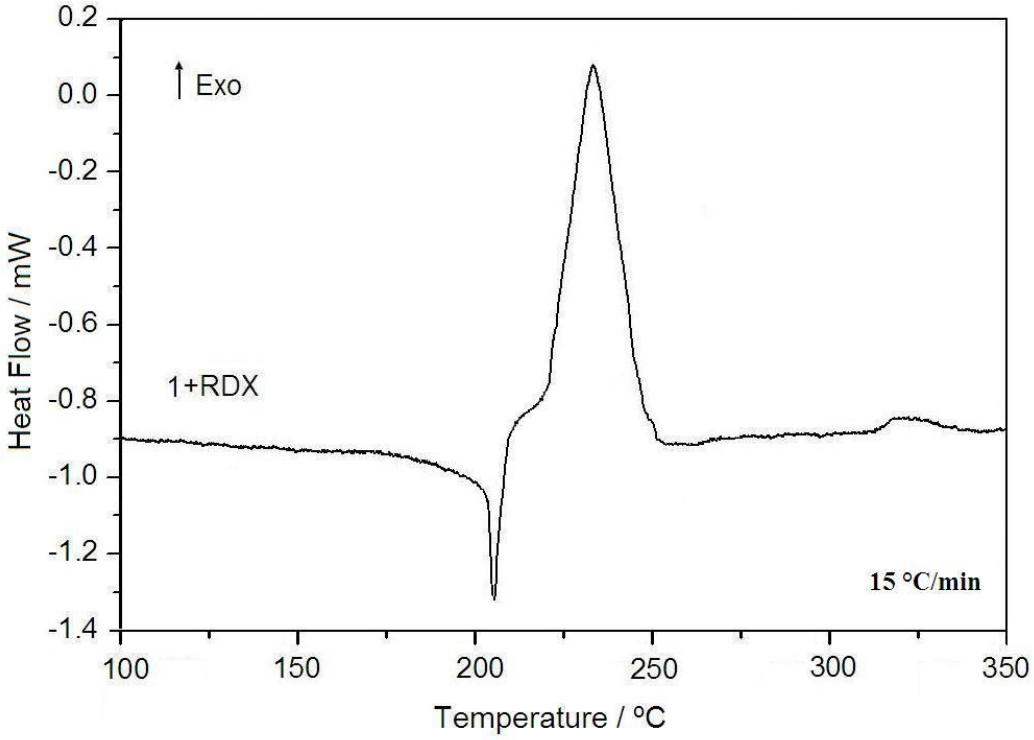

Fig. S15 DSC curve of complex **1** + RDX under the linear heating rate of 15 °C/min

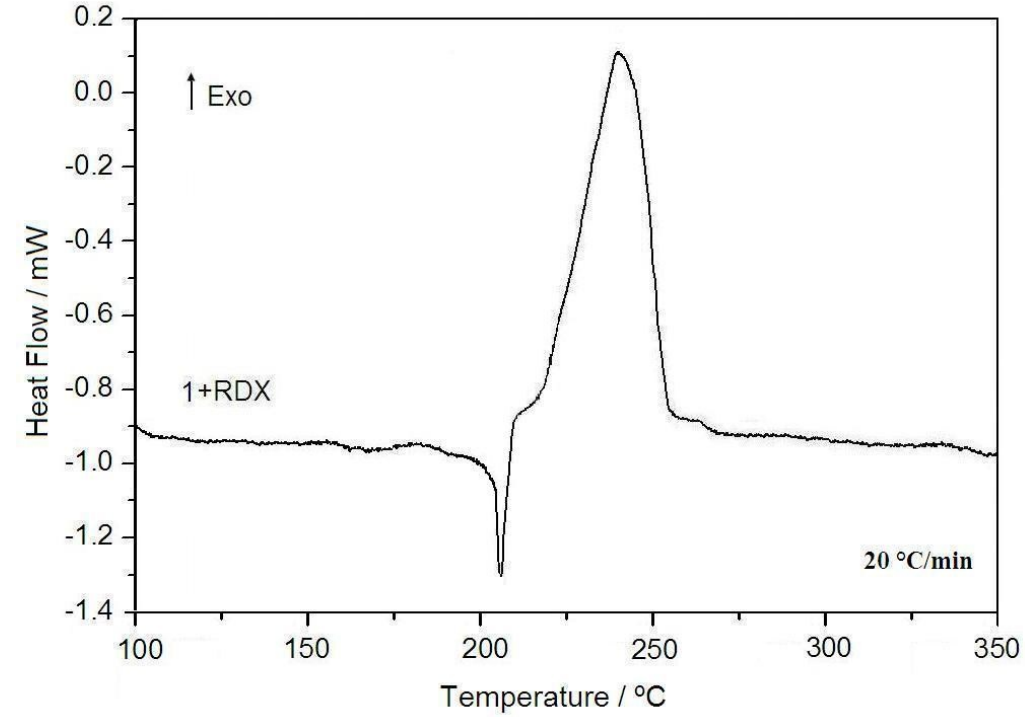

Fig. S16 DSC curve of complex **1** + RDX under the linear heating rate of 20 °C/min

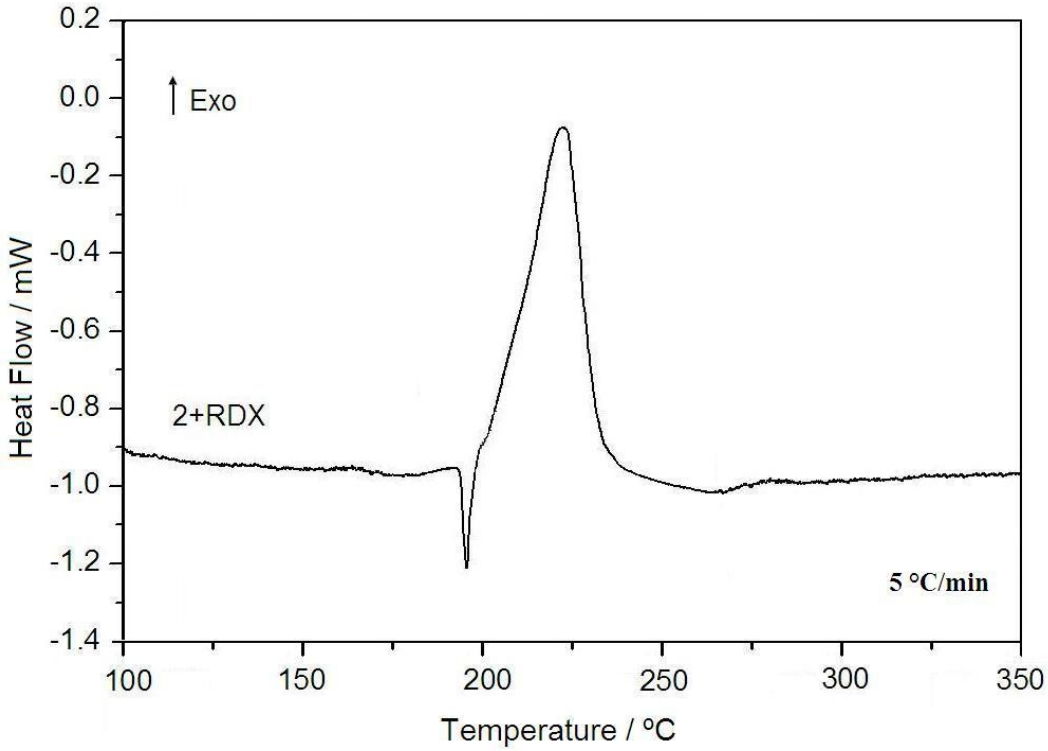

Fig. S17 DSC curve of complex **2** + RDX under the linear heating rate of 5 °C/min

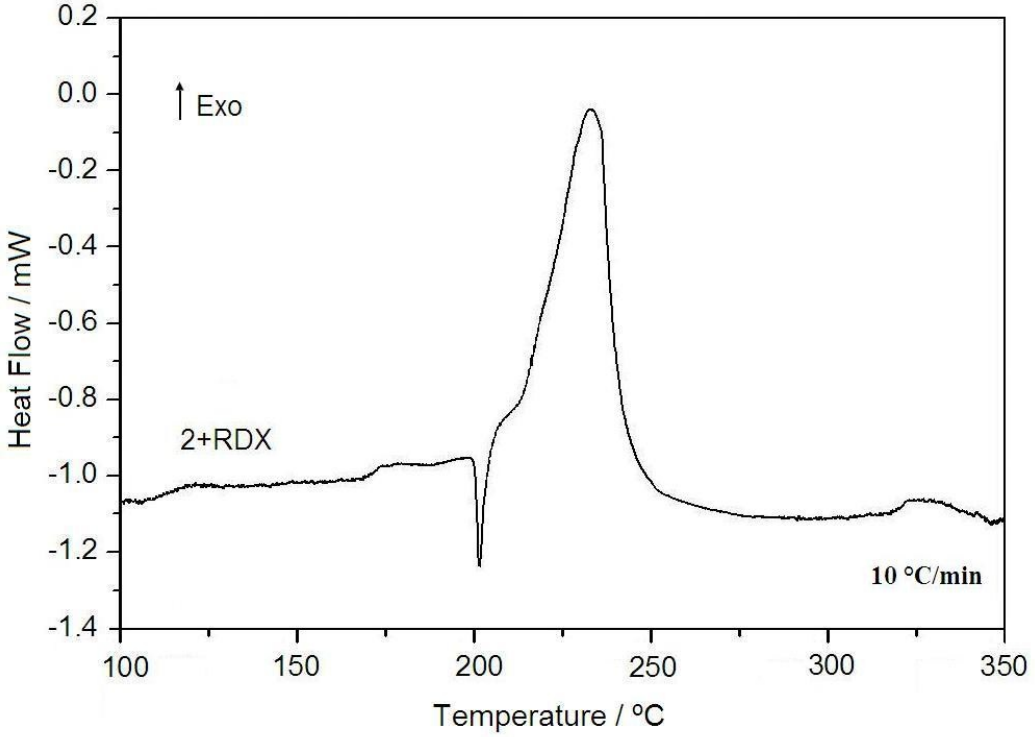

Fig. S18 DSC curve of complex **2** + RDX under the linear heating rate of 10 °C/min

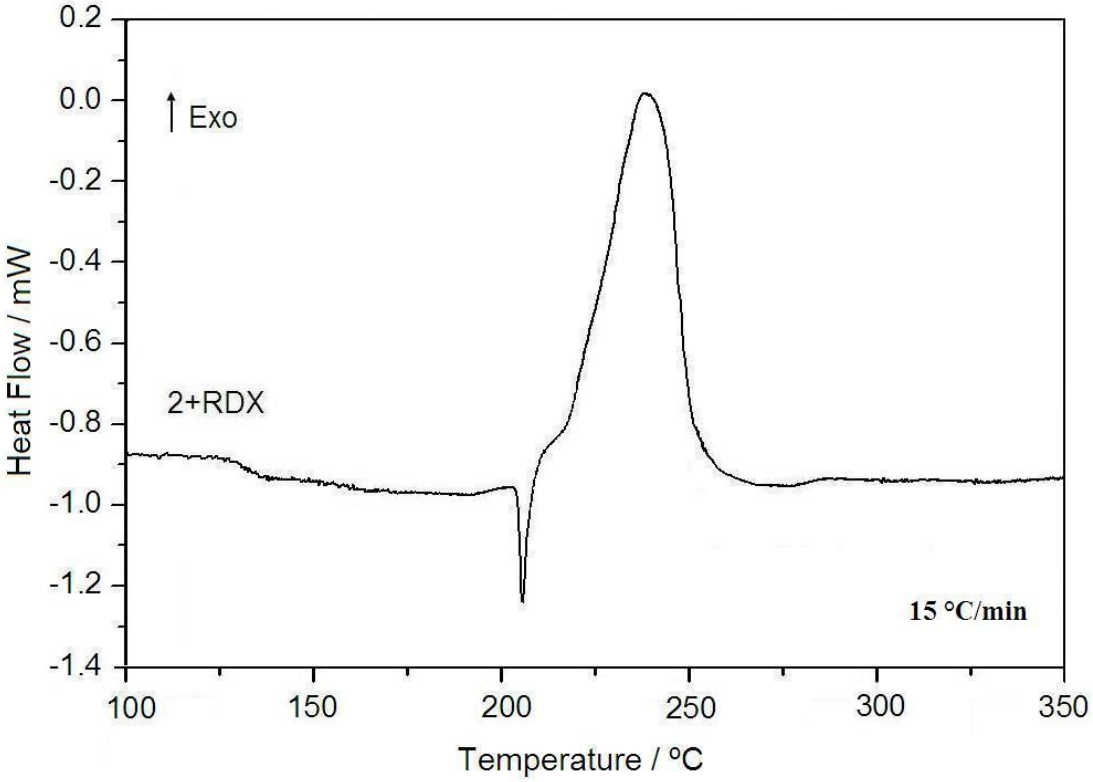

Fig. S19 DSC curve of complex **2** + RDX under the linear heating rate of 15 °C/min

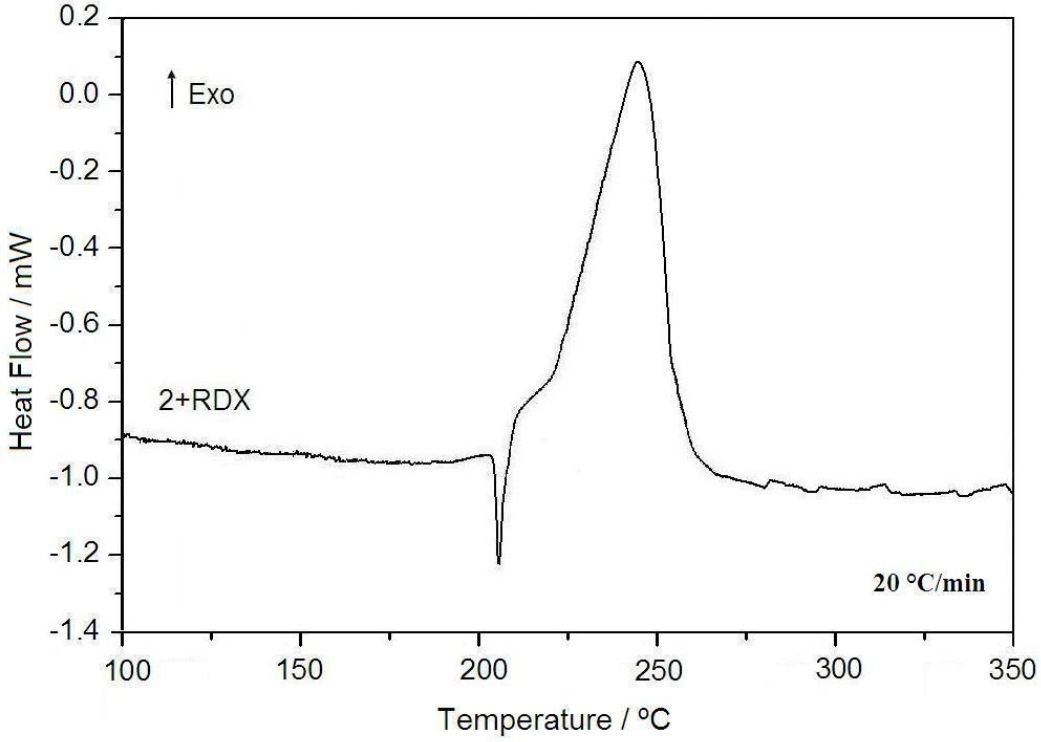

Fig. S20 DSC curve of complex **2** + RDX under the linear heating rate of 20 °C/min